THE ASTROPHYSICAL JOURNAL, 557:297–303, 2001 August 10

THE STATISTICS OF RADIO PULSARS: A SPARK MODEL

G. L. FAN,[1] K. S. CHENG,[1] AND R. N. MANCHESTER[2]
Received 2001 March 6; accepted 2001 April 12

ABSTRACT

We use Monte Carlo techniques to relate a theoretical pulsar emission model to the observed distributions of pulse period, magnetic field strength, distance, and luminosity of radio pulsars. We assume that the radio luminosity of pulsars is proportional to the gap potential and current flow from the polar cap. The current is assumed to be nonuniform and clustered in sparks, but only those sparks swept by the line of sight contribute to the observed radio luminosity. We test our model by using the Ruderman-Sutherland vacuum gap potential and find that the simulated distributions are consistent with those observed, with the exception of the period distribution. The model predicts more long-period pulsars than are observed. This discrepancy may result from the model itself, a reduced sensitivity of surveys to long-period pulsars, or the nondipole spin-down of pulsars.

Subject headings: pulsars: general — stars: neutron — stars: statistics

1. INTRODUCTION

Since the discovery of the radio pulsars (Hewish et al. 1968), there have been two types of statistical analyses used to understand their birth and evolution. In the first method, by Monte Carlo techniques, a model for the pulsar population is developed by making plausible assumptions for the initial properties of pulsars, their spatial distribution, and their evolution. Selection effects in pulsar surveys are then applied to derive the observed distributions of pulsar properties in order to compare the model with observations. The second method is to study the pulsar current as a function of period in order to calculate the birthrate and initial periods of pulsars (Vivekanand & Narayan 1981; Phinney & Blandford 1981). The pulsar-current approach is model free because it assumes nothing about the emission process or the nature of pulsar spin-down, but it is subject to large statistical uncertainties. Narayan (1987) attempted to improve the current analysis by replacing the apparent luminosities of the pulsars with model luminosities based on their period and period derivatives. At this point, the conclusions depend upon the assumed luminosity law. The Monte Carlo method is powerful except that it is model dependent. Several authors have used Monte Carlo techniques to investigate the properties of pulsars, such as the initial spin periods and the decay timescale for the magnetic field (see Gunn & Ostriker 1970; Stollman 1987b; Emmering & Chevalier 1989; Bhattacharya et al. 1992; Mukherjee & Kembhavi 1997). On the issues they studied, their results are inconclusive. Lorimer et al. (1993) believed that the main reason these papers give contrasting results lies in their choice of luminosity law. Obviously how the radio luminosity L_r depends upon the pulsar parameters (e.g., pulse period P, period derivative $\dot{P}$, or magnetic field B) plays a key role in the pulsar population modeling. So far there have been several attempts to connect the radio luminosity to P and $\dot{P}$. For example, in the pioneering statistical study of pulsar properties, Gunn & Ostriker (1970) proposed a model of pulsar evolution in which the magnetic field B decays exponentially with time and the radio luminosity is proportional to B^2, i.e., $L_r \propto B^2 \propto P\dot{P}$. Although this relation explained the observed period and age distributions well (Lyne, Manchester, & Taylor 1985), it was not a realistic luminosity model. Using the catalog of Manchester & Taylor (1981), two phenomenological relations were proposed: $L_{400} \propto P^{-1}\dot{P}^{-1/3}$ by Prószyński & Przybycien (1984) and $L_{400} \propto P^{-1.5}\dot{P}^{0.5}$ by Stollman (1987a), for $P^{-1.5}\dot{P}^{0.5} \leq 10\ \mathrm{s}^{-1.5}$, otherwise constant. Here $L_{400} \equiv S_{400}d^2$ is the radio luminosity at 400 MHz (in units of mJy kpc^2), S_{400} is the mean flux density measured at 400 MHz, and d is the distance to the pulsar. Emmering & Chevalier (1989) argued that the observed luminosity relation is affected by selection effects and therefore may not be an accurate representation of the intrinsic luminosity relation. They assumed a general relationship $L_r \propto P^{\alpha}\dot{P}^{\beta}$ with parameters α and β adjustable until a satisfactory agreement is obtained to the observed data. They found that $\alpha \approx -3\beta$, which means that young rapidly spinning pulsars are very bright, and therefore they required injection in order to account for the lack of such objects in the observed sample. Although the possible difference between the observed and the intrinsic luminosities has been considered, the relationship obtained by Emmering & Chevalier (1989) has no physical foundation, and in their simulations they took simple treatment of dynamics of pulsar evolution. In addition, the data set available at that time was based on a distance model that can be improved (Taylor & Cordes 1993). In Lorimer et al.'s (1993) paper concerning the investigation of the birthrate and initial spin periods of radio pulsars by the model-free approach, their least-squares fit to the updated data set, with luminosities derived using the Cordes et al. (1991) distance model, demonstrated that the dependence of the luminosity on period and period derivatives is weaker than has previously been estimated. They concluded that the large scatter of luminosities about the simple P-$\dot{P}$ power laws suggests that other factors affect the observed luminosity (e.g., geometric effects). Recently, Allen & Horvath (2000) revisited the issue of pulsar radio luminosity laws using the most recent data (Taylor, Manchester, & Lyne 1993), which was based on the most recent distance model of Taylor & Cordes (1993). They found no statistical support for the relation $L_r \propto B/P^2$ as Stollman (1987b) did.

[1] Department of Physics, University of Hong Kong, Hong Kong, People's Republic of China; fang@hkusua.hku.hk, hrspksc@hkucc.hku.hk.

[2] Australia Telescope National Facility, CSIRO, P.O. Box 76, Epping, NSW 1710, Australia; rmanches@atnf.csiro.au.

They fitted linear laws of the form $\log L_r = \alpha + \beta \log (B/P^2)$ to the data and found that β is smaller than Stollman's (1987a) value. It also depends sensitively on the binning procedure, besides being affected by the choice of catalog and the assumed threshold that defines "young" and "old" pulsars. Our conclusion is that at the present time, there appears to be no satisfactory luminosity law to account for the observed luminosities of pulsars.

Motivated by the current debate on radio luminosity laws used in the statistics of pulsars, in the present paper we try to connect theoretical pulsar emission models to the observed statistical properties of radio pulsars using Monte Carlo techniques. Although there are a wide range of theories for pulsars, it is generally believed that pulsar radiation originates from relativistic outgoing charged particles that are accelerated in a polar gap. From estimates of the brightness temperature, radio emission from pulsars is believed to be the result of coherent emission processes resulting from the interactions between the relativistic outgoing primary electrons/positrons and the secondary electron/positron pair plasma. There are two major types of models that describe gap formation and particle acceleration within the gap. The first type is the Arons & Sharleman (1979) space charge-limited model, in which the charged particles flow freely from the polar cap surface and form a steady outflow current. The particles are accelerated within a scale height of about one stellar radius $R \approx 10^6$ cm by the potential drop resulting from the curvature of field lines and/or inertia of the outstreaming particles. The second type is the Ruderman & Sutherland (1975, hereafter RS75) vacuum gap model, in which the free outflow from the polar cap surface is strongly impeded, leading to the formation of an empty gap just above the polar cap. When the potential drop of the empty gap is large enough, discharges (sparks) take place, and the outgoing charged particles are electrons/positrons produced in the sparks.

Both types of polar gap models have problems in accounting for the observed pulsar radio emission. In the stationary models, the inertial potential drop is not large enough to explain the entire population of observed pulsars. The gap models seem to account more naturally for characteristics of pulsar radio emission, but they face fundamental problems, principally the binding energy associated with gap formation itself (Hillebrands & Muller 1976; Flower et al. 1977; Kossl et al. 1988). Recently, the common conclusion that electron-positron pairs with high densities exist close to the neutron star has been questioned by several authors. Kunzl et al. (1998) considered the assumption of dense pair plasmas for the problem of radio wave propagation within the neutron star magnetosphere and found that the existence of low-frequency radio emission, e.g., from the Crab pulsar, is incompatible with the scenario of extended dense pair production. These findings were confirmed by the theoretical investigation of Melrose & Gedalin (1999). The simulations of the pair cascade by Arendt & Eilek (2000) for strong and weak magnetic fields revealed difficulties for an efficient production of secondary pairs by high-energy primary particles via γ-ray curvature photons, although their findings need more investigation. Taking both thermal and field emission processes into account, Jessner, Lesch, & Kunzl (2001) evaluated the conditions for e^- emission from pulsar surface for a simple Goldreich-Julian geometry, and their conclusion is that the conditions for magnetic pair production are not met anywhere along the field lines up to a height of 1500 pulsar radii. Leaving such debates around the theory of pulsar emission open, in this paper we explore the spark-associated model, namely the RS75 model, in terms of pulsar statistics by the Monte Carlo method. Stollman (1987a) has attempted to explain their two-population luminosity law in terms of the RS75 model. However, he just simply assumed that the luminosity is proportional to the potential drop. And if one adopts his threshold at 10^{13} Gs^{-2}, $\sim$80% of pulsars are necessarily "old," which does not seem reasonable (Allen & Horvath 2000). In this paper, we shall carefully consider the emission picture of the polar cap and those factors that will affect the luminosity we observe.

We assume that the radio luminosity L_r is proportional to the gap potential drop and current flow from the polar cap, i.e.,

$$L_r \propto \dot{N}_{\rm gap} e \Delta V_{\rm gap} , \tag{1}$$

where $\dot{N}_{\rm gap}$ is charged-particle flux from the polar cap and $\Delta V_{\rm gap}$ is the gap potential drop. According to the RS75 model, the high potential drop across the gap is discharged by the photon-induced pair creation in the strong and curved magnetic fields. The charges of opposite signs are accelerated in opposite directions to extremely relativistic energies and emit curvature photons whose energies exceed $2m_e c^2$, resulting in an $e^{\pm}$ pair avalanche. This cascade of pair production results in a "spark" breakdown of the gap. It is natural to interpret the plasma columns associated with these sparks as sources of emission from pulsars. We further assume that only those sparks that are randomly swept across by the line of sight contribute to the observed radio luminosity. Using this model for the intrinsic luminosity of pulsars, we perform Monte Carlo simulations to reproduce the statistical distributions of the period, surface dipole magnetic field, distance, and radio luminosity of pulsars and compare them with the observed data.

We present our model in § 2. The selection of the observed sample of radio pulsars is summarized in § 3. In § 4 we describe the Monte Carlo simulation used to generate the (model) Galactic pulsars. We present the simulated results and compare them with the observed distributions in § 5. A brief conclusion is given in § 6.

2. MODELS

According to the RS75 model, a polar gap spans the open field lines from the stellar surface up to an altitude h. The potential difference between the base and the top of the gap is given by

$$\Delta V = \frac{2\pi h^2}{c} \frac{B}{P} . \tag{2}$$

The height h of the gap is determined by the condition that it must be large enough for an electron/positron accelerated inside the gap to emit a curvature photon that can be converted to a pair within the gap. This condition gives

$$h = 5 \times 10^3 \rho_6^{2/7} P^{3/7} B_{12}^{-4/7} \text{ cm} , \tag{3}$$

$$\Delta V = 1.6 \times 10^{12} \rho_6^{4/7} P^{-1/7} B_{12}^{-1/7} \text{ V} , \tag{4}$$

where ρ_6 is the radius of curvature of the local magnetic field lines along which electrons/positrons move, in units of 10^6 cm. The gap continually breaks down (sparks) by forming electron-positron pairs. Each spark develops expo-

nentially until the plasma density ρ reaches a value close to the corotational Goldreich & Julian (1969) density ρ_{GJ}, when the potential drop within the spark filament is reduced to a value below the threshold for γ-B pair production and inhibits another simultaneous discharge within a distance of the order of h. The polar gap is thereby populated by a number of isolated sparks. Sparks supply corresponding plasma columns that can give rise to coherent radio emission and hence subpulses due to some instability developing above the gap. Recently, Deshpande & Rankin (1999) showed that drifting subpulses in PSR B0943+10 may be explained by circulating sparks, as originally proposed in the RS75 model; a similar model was proposed for PSR B0031−07 (Vivekanand & Joshi 1999). Gil & Sendyk (2000) estimated that both the dimensions of each spark and the separation of adjacent sparks are about the order of polar gap height, based on a general picture of pair creation in strong curved magnetic fields and dimensional analysis.

According to above picture, the total luminosity given by the sparks is

$$L_{\max} = N_{\rm sp} L_{\rm sp} , \tag{5}$$

where $N_{\rm sp}$ is the total number of sparks in the polar cap region, roughly estimated by

$$N_{\rm sp} \sim r_p^2/h^2 , \tag{6}$$

where r_p is the radius of polar cap. The term $L_{\rm sp}$ is the maximum luminosity generated by a single spark and can be expressed as

$$L_{\rm sp} = \dot{N}_{\rm sp} e \Delta V , \tag{7}$$

where $\dot{N}_{\rm sp} = \pi h^2 B/eP$ is the maximum particle flux developed in one spark. After the sparks leave the gap, the acceleration of the particles stops, and particles may suffer energy loss processes via curvature radiation and inverse Compton scattering before the instability occurs and they lose their remaining energy to coherent radio radiation. Therefore, equation (5) gives the maximum luminosity generated by sparks.

Observed radio luminosities have a wide scatter for given values of P and $\dot{P}$. There are a number of reasons why the observed luminosity may be lower than the maximum luminosity. The first is the randomness of the line of sight. Only the components (or sparks) swept by the line of sight contribute to the observed radio luminosity. A second is the uncertainty of the conversion efficiency of particle kinetic energy to radio radiation. A third arises from errors in the measured distances to pulsars. Finally, there is the uncertainty in the estimation of the total radio luminosity from the observed luminosity at 400 MHz. This conversion sensitively depends on the spectral index and the cutoff at low frequency. Taking these factors into consideration, we can derive the model luminosity at 400 MHz. In order to compare the model results and the observed data (L_{400}), we have noticed the conversion between the units of ergs^{-1} Hz^{-1} and mJy kpc^2 and define the model luminosity at 400 MHz (in units of mJy kpc^2) as

$$L_{400,\rm model} = L_{\rm model}(400\ {\rm MHz})/400\ {\rm MHz} , \tag{8}$$

where

$$L_{\rm model}(400\ {\rm MHz}) = \eta_{400} N_{\rm eff} L_{\rm sp} . \tag{9}$$

Here $N_{\rm eff}$ is the number of swept components, randomly chosen between 1 and $N_{\max}$; $N_{\max}$ is the maximum number of sparks along the diameter of polar cap,

$$N_{\max} \sim r_p/h ; \tag{10}$$

η_{400} is a random function resulting from the uncertainties due to (1) the conversion efficiency from particle energy to radio radiation, (2) the uncertainty in pulsar distance, and (3) the conversion from radio luminosity to $L_{\rm model}$ (400 MHz). We assume that $\log \eta_{400}$ satisfies a Gaussian distribution,

$$\rho_{\eta_{400}}(\log \eta_{400}) = \frac{1}{\sqrt{2\pi}\sigma_{\eta_{400}}} \times \exp\left[-\frac{1}{2}\left(\frac{\log \eta_{400} - \langle \log \eta_{400}\rangle}{\sigma_{\eta_{400}}}\right)^2\right], \tag{11}$$

with $\langle \log \eta_{400}\rangle$ and $\sigma_{\eta_{400}}$ as fitted parameters. We point out that whether the pulsar beam is a nested cone structure (RS75; Rankin 1993; Gil & Krawczyk 1996; Gil & Sendyk 2000) or a patchy structure (Lyne & Manchester 1988; Manchester 1995; Tauris & Manchester 1998; Han & Manchester 2001) makes no difference to the model; in both cases the line of sight randomly cuts through a number of sparks. We use equations (7)–(11) to generate the distribution of pulsar radio luminosity at 400 MHz. Whether or not the pulsar will be observed depends on the sensitivity of individual pulsar surveys. This will be discussed in § 4.

There is growing evidence that the surface magnetic field of pulsars is dominated by a multipole magnetic field, as was implicitly assumed in the RS75 model to explain the copious pair production process. The bolometric polar cap radii inferred from blackbody fits to thermal pulsed X-ray emission and the known distance to the pulsars (e.g., PSRs B1929+10, B0950+08, B0656+14, B1055−52, J0437−4715; Greiveldinger et al. 1996) are much smaller than the canonical radius corresponding to a purely dipole field:

$$r_p = \left(\frac{2}{3}\right)^{3/4} R\left(\frac{\Omega R}{c}\right)^{1/2} \approx 10^4 P^{-1/2}\ {\rm cm} . \tag{12}$$

The effective decrease in polar cap radius resulting from a multipolar field structure can be expressed in the form

$$r_{p,m} = b^{-1/2} r_p , \tag{13}$$

where $b = B_s/B_d$, and B_s is the surface field strength and B_d is the dipole magnetic field. A strong local magnetic pole within the polar cap region is assumed by Gil & Sendyk (2000) to drive spark discharges in the first place and to give a persistent spark arrangement in the form of a quasi-annular pattern, leading to a nested cone structure of the pulsar beam. However, a superstrong magnetic field ($B \geq 10^{14}$ G) will completely quench the radio emission due to the photon-splitting ($\gamma \rightarrow \gamma\gamma$) process, which competes with the pair production process at very high fields (Baring & Harding 1997). Therefore, we choose b between 1 and 10 and require that B_s is less than 10^{14} G.

3. OBSERVED SAMPLE OF NORMAL RADIO PULSARS

From the updated database available at the Australia Telescope National Facility, we select pulsars observed by at least one of three major surveys conducting at 400 MHz, the Parkes 70 cm survey (Lyne et al. 1998), and the Princeton NRAO survey phase I (Dewey et al. 1985) and phase

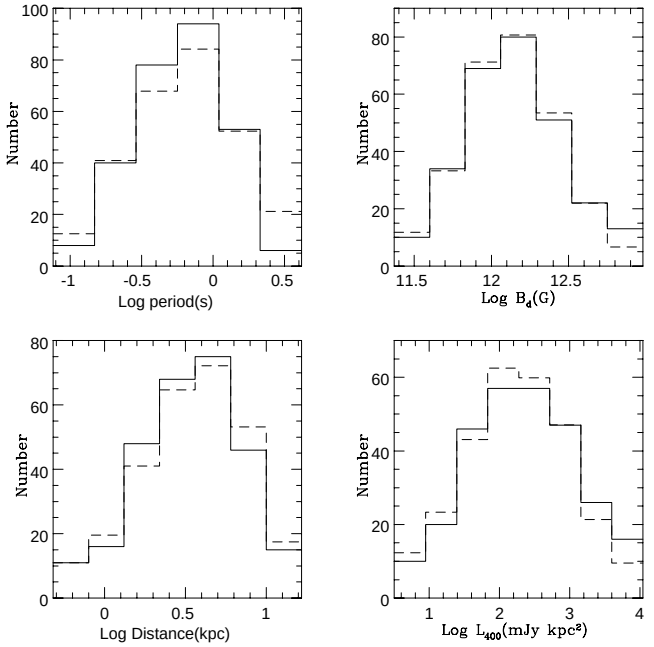

FIG. 1.—Comparison of the distributions of pulsar periods, magnetic fields, distances, and radio luminosities. *Solid lines*, the observed pulsars; *dashed lines*, the simulated pulsars. For the plots, the number of simulated pulsars is normalized to the same total as the real pulsars.

II (Stokes et al. 1986). These surveys cover the northern and southern sky and detected a total of 403 pulsars, providing a large sample suitable for statistical analyses. We drop a pulsar if (1) its distance is greater than 20 kpc, since such distances are very uncertain and/or the pulsar may not be in the Galaxy, (2) its age is greater than 2×10^7 yr because we want to avoid dealing with the complicated and controversial magnetic field decay problem, and (3) its $\dot{P}$ is not available. We obtained 206 pulsars from the Parkes 70 cm survey and 106 pulsars from Princeton NRAO survey phases I and II, giving a final combined observed sample of 279 pulsars. The logarithm distributions of period, dipole magnetic field, distance, and luminosity at 400 MHz of the selected observed sample are displayed in Figure 1.

4. MONTE CARLO SIMULATION OF GALACTIC PULSARS

In our Monte Carlo simulations, we create pulsars with random ages less than 2×10^7 yr. The birth location for each pulsar is drawn from two independent distributions in z, the direction perpendicular to the Galactic disk, and R, the distance to the Galactic center in the plane of the Galaxy. The z distribution is taken to be an exponential disk with a scale height of 75 pc. The radial distribution has the form $R \exp(-R/R_{\rm exp})$, where $R_{\rm exp} = 4.5$ kpc (Paczynski 1990). The initial velocity of each pulsar is the vector sum of the circular rotation velocity and a random velocity produced from the supernova explosion. The rotation velocity is calculated from the local gravitational potential, where $v_{\rm rot} = [R(\partial\phi_{\rm grav}/\partial R)]^{1/2}$. The random velocity satisfies Maxwellian distribution following the results of Lorimer, Bailes, & Harrison (1997). We use the Galactic gravitational potential given in Paczynski (1990).

The period of each pulsar at time t is calculated assuming a 90° inclination angle and that magnetic dipole radiation energy losses dominate, i.e., $P(t) = (P_0^2 + 1.95 \times 10^{-39} B_d^2 t)^{1/2}$, where P_0 is the initial rotation period. The initial period distribution P_0 is not well known but is not critical, and we fix it at $P_0 = 0.1$ s following Bhattacharya et al. (1992). The term B_d is the dipole magnetic field of the pulsars and is assumed to be distributed as a Gaussian in $\log B_d$, and we have assumed that the magnetic fields of pulsars do not decay on timescales smaller than 10^7 yr (see Bhattacharya et al. 1992). As discussed in § 2, we modify the surface multipole magnetic field B_s by $B_s = bB_d$. We randomly choose b between 1 and 10, but we require B_s to not be greater than 10^{14} G. The possible values of the radius of curvature (in units of 10^6 cm) of the local multipole magnetic field lines are taken to be in the range $0.1 \le \rho_6 \le 1$, reflecting the natural characteristic size scales such as the neutron star radius $R \sim 10^6$ cm, the thickness of the stellar crust, and the polar cap radius $r_p \sim 3 \times 10^4$ cm. We use equations (7)–(11) to calculate the pulsar radio luminosity at 400 MHz in order to compare with the observed data.

For a pulsar to be observed, its flux density at the Earth must be greater than the sensitivity threshold of the survey. For this to be the case, its radio beam must be directed toward us. We adopt the period-dependent radio beamwidth model of Biggs (1990), i.e., $w = 6.^\circ 2 P^{-1/2}$, where w is the half-angle of the radio emission cone. The radio beaming fraction can be expressed as

$$f_r(w) = (1 - \cos w) + \left(\frac{\pi}{2} - w\right) \sin w \,, \qquad (14)$$

where a random distribution of magnetic inclination angles is assumed (Emmering & Chevalier 1989). Then, following Emmering & Chevalier (1989), a sample pulsar with a given period is chosen in one out of $f_r(p)^{-1}$ cases using the Monte Carlo method.

We simulate Parkes 70 cm survey and Princeton NRAO survey phases I and II (Manchester et al. 1996; Dewey et al. 1985; Stokes et al. 1986). The principal survey parameters are listed in Table 1, where ν is the observing frequency, $\tau_{\rm samp}$ is the sampling interval, $\Delta\nu$ is the channel bandwidth, and $S_{\rm min}$ is the survey sensitivity for long-period low dispersion measure pulsars and low background temperature. We use the model of Taylor & Cordes (1993) to calculate the dispersion measure. The sky temperature is obtained from Haslam et al. (1982) and scaled to observing frequencies using a -2.6 power law of frequency dependence (Johnston et al. 1992). Pulsars for which energy flux $L_{400,\rm model}/d^2$ is above the threshold of the survey are considered to be radio-detectable pulsars.

5. SIMULATION RESULTS

We use the Monte Carlo method to generate 2×10^6 pulsars with ages lower than 20 million years. The initial values of period, position, velocity, and magnetic field strength of each pulsar were determined by the random selection processes described in § 4. They are evolved to the present time according to the relations described in § 4.

TABLE 1

VALUES OF SURVEY PARAMETERS

Survey	ν (MHz)	$\tau_{\rm samp}$ (ms)	$\Delta\nu$ (MHz)	$S_{\rm min}$ (mJy)	Declination (deg)
Parkes 70	436	0.3	0.125	3	0
NRAO phase I.....	390	16.67	2	2	−18
NRAO phase II.....	390	2.0	0.25	3	−18

Once the present period and magnetic field are determined, the radio luminosity is then calculated as described in § 2. Those pulsars that are found to be detectable constitute the simulated sample. We use the bin-free Kolmogorov-Smirnov (K-S) test and the bin-dependent χ^2 test to compare the simulated and observed populations.

We use the random number generator described in Press et al. (1992). Since our simulations involve generation of a very large number of pulsars, we take special care to test the stability and optimization of the random number generator. We found that the simulated results are subject to statistical fluctuation; i.e., the properties of the pulsars generated by using one set of random numbers will be different from those generated by using another set of random numbers. We checked that such fluctuations do not prevent us from making general conclusions, although the quantitative results we present are a rough estimate.

For convenience, we have fixed some of the parameters in our simulation, such as the initial period, the scale height of birth location, and the width of initial velocity. The simulation parameters that we allow to vary are $\log B_{d0}$, σ_B, $\langle \log \eta_{400} \rangle$, and $\sigma_{\eta_{400}}$. We vary $\log B_{d0}$ from 12.3 and σ_B from 0.3, both in steps of 0.02. For fixed $\log B_{d0}$ and σ_B, $\langle \log \eta_{400} \rangle$ and η_{400} are adjusted to get the best fit to distributions of distance and radio luminosity at 400 MHz of observed sample. Here we have used K-S tests to perform the search. We take the "agreement" between distributions of simulated and observed samples if the K-S probabilities are greater than 0.1, which means that both observed and simulated data sets are drawn from the same parent distribution. Finally, K-S tests and χ^2 tests (Press et al. 1992) were done on the distributions of four pulsar properties, namely, the distributions of the pulse period (P), the dipole magnetic field (B_d), the distance (d), and the radio luminosity at 400 MHz (L_{400}).

We get the best fits to four observed distributions at $\log B_{d0} = 12.38$, $\sigma_B = 0.32$, $\langle \log \eta_{400} \rangle = -3.3$, and $\sigma_{\eta_{400}} = 0.91$, although we found that these four parameters can vary in acceptable ranges in which we may find compatible values to satisfy our "agreement" standard. The acceptable range of $\log B_{d0}$ is from 12.34 to 12.42, σ_B from 0.32 to 0.36, and $\sigma_{\eta_{400}}$ from 0.8 to 1.0, while $\langle \log \eta_{400} \rangle$ varies from -3 to -4. Figures 1 and 2 show the bin and cumulative of the observed pulsars against the simulated pulsars corresponding to $\log B_{d0} = 12.38$, $\sigma_B = 0.3$, $\langle \log \eta_{400} \rangle = -3.3$, and $\sigma_{\eta_{400}} = 0.91$. The K-S and χ^2 test results for four distributions, ($\log P$), ($\log B_d$), ($\log d$), and ($\log L_{400}$), are shown in Table 2. For the χ^2 test, we normalize the number of simulated pulsars to the same total as for the real sample. The bins used in the χ^2 tests are the same as those shown in Figure 1. We bin the data into equal step sizes except for the first and last bins in which we keep the numbers at about 10 to improve the statistics. The number of degrees of freedom is therefore the number of bins minus two. For the K-S test, $D_{\max}$ is the maximum difference between cumulative distribution functions corresponding to the observed and simulated data. The hypothesis that model and observed pulsars are drawn from the same parent population can be rejected at the greater than 90% level if $D_{\max} > 0.075$. Using these statistical tests, it is seen from Table 2 that both the χ^2 and the K-S test results indicate that three out of four distributions are very good fits. However, the model period distribution is not a very good representation of the observed distribution.

TABLE 2

TEST RESULTS

	K-S TEST RESULTS		χ^2 TEST RESULTS	
DISTRIBUTION	$D_{\max}$	Prob (%)	χ^2	Prob (%)
log P (s)	0.073	11.41	15.13	0.44
log B_d (G)	0.045	66.42	3.65	60.15
log D (kpc)	0.050	52.00	3.43	63.35
log L_{400} (mJy kpc^2).....	0.055	39.39	7.13	30.94

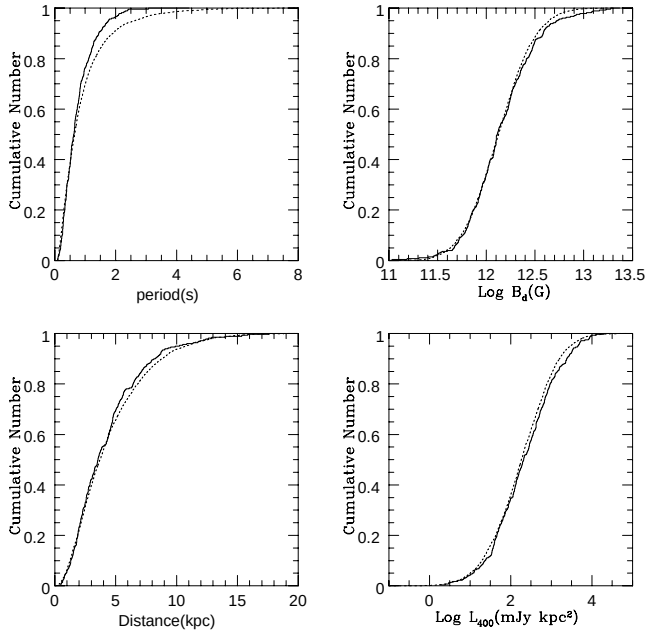

FIG. 2.—Normalized cumulative distributions for the observed pulsars (*solid curves*) compared with the distributions of the simulated pulsars (*dotted curves*).

From Figures 1 and 2, we can see that compared to the observed period distribution, the model predicts more long-period pulsars, especially with $P > 2$ s. Among the total 403 pulsars that we use as our original database, there are 17 pulsars with periods greater than 2 s. We drop only four of them because their ages are above 2×10^7 yr. The χ^2 test for the left five bins of the period comparison gives $\chi^2 = 4.29$, prob(χ^2, 3) = 23.20%, implying a good fit.

We suggest several possibilities that could lead to such a discrepancy. First, the model luminosity generated as described in § 2 may not be suitable for long-period pulsars. Adopting $N_{\max}$ instead of $N_{\rm eff}$ in equation (9), we obtain the model luminosity $L_{400}^{\rm model} \propto P^{-17/14} B_s^{2/7}$, i.e., $L_{400}^{\rm model} \propto P^{-1.07} \dot{P}^{0.14}$, which is a weaker relation between L and $P\dot{P}$ than previously proposed (Gunn & Ostriker 1970; Prószyński & Przybycien 1984; Stollman 1987b; Emmering & Chevalier 1989; Lorimer et al. 1993). Even this relationship will be scattered by the uncertainties of observed $N_{\rm eff}$, the conversion efficiency to radio radiation, etc. This law may represent well the luminosity for most pulsars but will lead to the insufficient decrease of luminosity for long-period pulsars. We therefore suggest that there may exist other factors that will decrease the luminosity of old pulsars. Second, the model for the calculation of $S_{\min}$ may be deficient for long-period pulsars. Extra factors such as

interference may reduce the sensitivity of surveys at large periods, and unmodeled hardware and software cutoffs may be important. Third, we have assumed that the model pulsar spin-down is due to pure dipole radiation, which implies a braking index of 3.0. Plate tectonic models (Ruderman, Zhu, & Chen 1998) suggest that the braking index of young pulsars should be less than that for dipole radiation but that it becomes larger than 3.0 when the pulsars age, which means for aged pulsars it will take much longer to evolve to the current period. This may explain the discrepancy between the model results and the observed data in the period distribution, especially in the long period range.

The factor η_{400}, which is the ratio of 400 MHz radio luminosity to spark luminosity, is about $10^{-3.3}$. If we assume a typical pulsar spectral index of -1.6 (Lorimer et al. 1995) and a minimum radio frequency of 50 MHz, the total energy of the radio radiation is about $10^{-2.5}$ of the particle energy. In addition, the mean pulsar profile is an integration by adding many individual pulses, and we would probably see only parts of a spark rather than the full one; the averaged intensity of each component may decrease by a factor of at least ~ 0.25 owing to the drifting and the spacing among such two-dimensional sparks. Therefore, we estimate the real conversion efficiency from the particle kinetic energy to the radio radiation to be at least 1%.

The standard deviation of $\log \eta_{400}$, $\sigma_{\eta_{400}}$, is about 0.9. Variations in the conversion efficiency also include the uncertainty in the measurement of pulsar distance and the randomness in the number of sparks traversed by the line of sight. Taylor & Cordes (1993) believe that their new model provides distance estimates accurate to $\sim 25\%$ or better. There is easily a factor of 0.3 in variation in both conversion efficiency and number of sparks cut through by the line of sight. The combined variation of these three factors can easily account for $\sigma_{\eta_{400}}$.

6. CONCLUSIONS

We have emphasized that it is not possible to directly compare the theoretical predictions to the observed data. There are at least four uncertainties affecting the observed values, namely, the distances to pulsars, the randomness of number of sparks being observed or equivalently what fraction of emission region being observed, the randomness of conversion efficiency from particle kinetic energy to radio radiation, and the ratio between the monochromatic luminosity (at 400 MHz) and the luminosity for the entire radio band. In this paper, we adopt a Monte Carlo approach, which can take into account at least three of these uncertainties by introducing Gaussian distribution functions. Since the main purpose of our work is to connect a theoretical pulsar model to the statistics of radio pulsars, the intrinsic luminosity used in the simulations is given by the model instead of being given by the phenomenological relations derived from the observed data. We assume that the radio luminosity of a pulsar is proportional to the gap potential and the current flow in the polar cap. The proportionality constant is assumed to have a Gaussian distribution to take into account the uncertainties.

In the sample selection, we are careful to choose a uniform sample for the statistical analysis. We use a Monte Carlo method to generate a model pulsar population in the Galaxy. After applying the observational selection effects to our model pulsar population, we compare our model distributions in period, magnetic field, distance, and luminosity with the observed distributions. Except for the period distribution, they agree well. Specifically, we generate more long-period pulsars in our model population than are found in the observed population. We speculate that this may result from the following: (1) the theoretical model (RS75) we choose may not work very well for long-period pulsars, (2) the sensitivity of surveys may be lower for longer period pulsars, and/or (3) pulsars spin down more slowly than predicted by dipole radiation when pulsars age as suggested by the plate tectonic model (Ruderman et al. 1998).

We thank the referee M. Kramer for his very careful reading of the paper and his many useful suggestions. We are grateful for discussions with Professor J. A. Gil and Dr. L. Zhang during the initial stages of the project. We acknowledge Q. R. Zheng for helpful discussions regarding statistics. This work is partially supported by an RGC grant of Hong Kong Government and the Croncher Foundation Senior Research Fellowship of the University of Hong Kong. The Australia Telescope is funded by the Commonwealth of Australia for operation as a National Facility managed by CSIRO.

REFERENCES

Allen, M. P., & Horvath, J. E. 2000, MNRAS, 317, 23
Arendt, P. N., & Eilek, J. A. 2000, in IAU Colloq. 177, Pulsar Astronomy: 2000 and Beyond, ed. M. Kramer, N. Wex, & R. Wielebinski (San Francisco: ASP), 445
Arons, J., & Sharleman, E. T. 1979, ApJ, 231, 854
Baring, M. G., & Harding, A. 1997, ApJ, 482, 372
Bhattacharya, D., Wijers, R. A. M. J., Hartman, J. W., & Verbunt, F. 1992, A&A, 254, 198
Biggs, J. D. 1990, MNRAS, 245, 514
Cordes, J. M., Weisberg, J. M., Frail, D. A., Spangler, S. R., & Ryan, M. 1991, Nature, 354, 121
Deshpande, A. A., & Rankin, J. M. 1999, ApJ, 524, 1008
Dewey, R. J., et al. 1985, ApJ, 294, L25
Emmering, R. T., & Chevalier, R. A. 1989, ApJ, 345, 931
Flower, E. G., et al. 1977, ApJ, 215, 291
Gil, J., & Krawczyk, A. 1996, MNRAS, 280, 143
Gil, J., & Sendyk, M. 2000, ApJ, 541, 351
Goldreich, P., & Julian, H. 1969, ApJ, 157, 869
Greiveldinger, C., et al. 1996, ApJ, 465, L35
Gunn, J. E., & Ostriker, J. P. 1970, ApJ, 160, 979
Han, G. L., & Manchester, R. N. 2001, MNRAS, 320, L35
Haslam, C. G., Salter, C. J., Stoffel, H., & Wilson, W. E. 1982, A&AS, 47, 1
Hewish, A., Bell, S. J., Pilkington, J. D., Scott, P. F., & Collins, R. A. 1968, Nature, 217, 709
Hillebrands, W., & Muller, E. 1976, ApJ, 207, 589
Jessner, A., Lesch, H., & Kunzl, T. 2001, ApJ, 547, 959
Johnston, S., Lyne, A. G., Manchester, R. N., Kniffen, D. A., D'Amico, N., Lim, J., & Ashworth, M. 1992, MNRAS, 255, 401
Kossl, D., Wolff, R. G., Muller, E., & Hillebrand, W. 1988, A&A, 205, 347
Kunzl, T., Lesch, H., Jessner, A., & Hoensbroech, A. 1998, ApJ, 505, L139
Lorimer, D. R., Bailes, M., Dewey, R. J., & Harrison, P. A. 1993, MNRAS, 263, 403
Lorimer, D. R., Bailes, M., & Harrison, P. A. 1997, MNRAS, 289, 592
Lorimer, D. R., Yates, J. A., Lyne, A. G., & Gould, D. M. 1995, MNRAS, 273, 411
Lyne, A. G., & Manchester, R. N. 1988, MNRAS, 234, 477
Lyne, A. G., Manchester, R. N., & Taylor, J. H. 1985, MNRAS, 213, 613
Lyne, A. G., et al. 1998, MNRAS, 295, 743
Manchester, R. N. 1995, JApA, 16, 107
Manchester, R. N., & Taylor, J. H. 1981, AJ, 86, 1953
Manchester, R. N., et al. 1996, MNRAS, 279, 1235
Melrose, D. B., & Gedalin, M. E. 1999, ApJ, 521, 351
Mukherjee, S., & Kembhavi, A. 1997, ApJ, 489, 928
Narayan, R. 1987, ApJ, 319, 162

Paczynski, B. 1990, ApJ, 348, 485
Phinney, E. S., & Blandford, R. D. 1981, MNRAS, 194, 137
Press, W., Flannery, B., Teukolsky, S., & Vetterling, W. 1992, Numerical Recipes: The Art of Scientific Computing (2d ed.; Cambridge: Cambridge Univ. Press)
Prószyński, M., & Przybycien, D. 1984, in Proc. Green Bank Workshop on Millisecond Pulsars, ed. S. P. Reynolds & D. R. Stinebring (Green Bank: NRAO), 151
Rankin, J. M. 1993, ApJ, 405, 285
Ruderman, M. A., & Sutherland, P. G. 1975, ApJ, 196, 51
Ruderman, M. A., Zhu, T., & Chen, K. 1998, ApJ, 492, 267
Stokes, G. H., et al. 1986, ApJ, 311, 694
Stollman, G. M. 1987a, A&A, 171, 152
———. 1987b, A&A, 178, 143
Tauris, T. M., & Manchester, R. N. 1998, MNRAS, 298, 625
Taylor, J. H., & Cordes, J. M. 1993, ApJ, 411, 674
Taylor, J. H., Manchester, R. N., & Lyne, A. G. 1993, ApJS, 88, 529
Vivekanand, M., & Joshi, B. C. 1999, ApJ, 515, 398
Vivekanand, M., & Narayan, R. 1981, JApA, 2, 315